PHYSICAL REVIEW A VOLUME 58, NUMBER 4 OCTOBER 1998

# Collision-induced dissociation of $CO_2^+$ ions

V. R. Bhardwaj, D. Mathur, and K. Vijayalakshmi
*Tata Institute of Fundamental Research, Homi Bhabha Road, Mumbai 400 005, India*

P. Hvelplund, M. O. Larsson, and C. P. Safvan
*Institute of Physics and Astronomy, University of Aarhus, DK-8000 Aarhus C, Denmark*

(Received 2 March 1998)

Collision-induced dissociation experiments have been conducted on $CO_2^+$ ions using three types of ion sources, different collision energies, light and heavy targets, and three different apparatuses possessing different values of energy and angular resolution. Results of all these collision experiments establish that collision-induced dissociation dynamics is remarkably different from that obtained in photoionization experiments. Although the $O^+ + CO$ channel is the energetically lowest dissociation pathway, dissociation into $CO^+ + O$ is found to be the preferred channel. Our measurements of the ratio $CO^+$ to $O^+$ are substantially higher than that obtained in photoionization experiments. Determinations of kinetic energies released upon dissociation of $CO_2^+$ are also made. Rationalization of our results is attempted in terms of curve crossings of low-lying excited states of $CO_2^+$ ions. [S1050-2947(98)13109-8]

PACS number(s): 34.20.−b, 34.50.Gb, 31.15.Ar, 33.15.Fm

## I. INTRODUCTION

In the past two decades the $CO_2$ molecule has attracted much attention, primarily due to the importance of both the neutral and the ionized form in nuclear and laser technologies and in studies of terrestial and planetary atmospheres [1–3]. Various techniques have been used to study the structure and fragmentation dynamics of this molecule. Dissociative ionization of $CO_2$ resulting in $O^+$ and $CO^+$ fragments has been studied by photoionization mass spectrometry [1,4,5]. The photoelectron-photoion coincidence technique has been used to probe state-selected dissociation dynamics [4]; the competition between dissociation and ionization of $CO_2$ has been investigated using intense, picosecond laser fields [6,7]. The relative abundances of the $O^+$and $CO^+$ fragments have also been studied in low-energy electron-impact experiments [8]. Collision-induced dissociation (CID), which has been a widely used ion-molecule collision technique for structure determination and fragment pathway analysis [9–12], has also been useful in identifying the electronic states of the dissociation products of $CO_2^+$ [13].

The fragments $O^+$ and $CO^+$ cannot be produced by direct ionization of the neutral molecule since the appropriate Franck-Condon factors are such that the dissociation continua of the $X$, $A$, and $B$ electronic states of $CO_2^+$ are not accessible by vertical ionization from the ground state of the neutral molecule. This was established by the absence of any peak in the $CO_2$ photoelectron spectrum [5] near the appearance thresholds for $O^+$ and $CO^+$ fragments (19.07 and 19.466 eV, respectively, as measured experimentally as well as deduced from thermochemical data). The next ionic state, $C$, lies above the dissociation limit for $O^+$+CO and, hence, fully predissociates. This was directly established by photoion-photoelectron coincidence measurements carried out by Eland [4]. *Ab initio* calculations of the potential energy surfaces of the ground and excited electronic states of $CO_2$ and its singly charged ion have been carried out by many researchers with varying degrees of success [14–18]. Configuration interaction (CI) calculations of Praet *et al.* [18], who obtained vertical ionization and excitation energies that are in reasonably good accord with experimental values [19], have provided the most detailed information on the dissociation mechanism of the $CO_2^+$ molecular ion.

The results of all recent calculations agree that the lowest-energy pathway for dissociation favors the formation of $O^+ + CO$ fragments. From the experimental viewpoint, at least as far as noncollision experiments are concerned, the measured ratio of $CO^+$ to $O^+$, which should be equal to the ratio of the populations of vibrationally excited levels of the fully predissociating $C$ state to the population of the ground state, has been found to be around 0.3 [4,20,21]. It is of interest to note that this value is actually close to the value expected if one assumes that *all* of the $CO_2^+$ ions in states that lie above the lowest-energy dissociation limit yield $CO^+$ [21] (in other words, if one assumes that once the threshold for $CO^+$ formation is crossed, $O^+$ ions are completely quenched). The complete quenching of $O^+$ ions in such cases has been rationalized by invoking curve crossing models (see, for instance, the extensive discussion in Praet *et al.* [18], and references therein).

Does this picture hold when dissociation is induced by collisions? We have attempted to address this question by studying the dissociation dynamics of $CO_2^+$ ions undergoing collisions with targets of various masses, like He, $N_2$, and $C_{60}$ at impact energies of 1–3 keV and also at 50 keV. No differences were found in the translational energy spectra of the dissociation products obtained using different target gases, and for comparative purposes we focus attention, in what follows below, only on the spectra obtained with He. The major finding we report here is that the measured ratio of $CO^+$ to $O^+$ was much higher in our experiments (significantly larger than unity) than what has been observed in photoionization experiments where $O^+$ is the more abundant fragment ion. This ratio was determined using three different translational energy spectrometers, each of which employed a different type of ion source to account for different degrees of internal excitation (vibrational and rotational energy) of the precursor ion. Low and high collision energies were employed to account for any possible instrumental factors related to angular acceptance angles that might affect the efficiencies with which different fragment ions were energy analyzed. Irrespective of the target gases used and the incident translational energy of the $CO_2^+$ ions, the ratio was found to be the same. There is evidence to suggest that the measured $CO^+$ to $O^+$ ratio is independent of the degree of the internal excitation of the precursor $CO_2^+$ ions. CID experiments in general, and meaurement of fragment ion ratios in particular, are instrinsically difficult to perform because of the conflicting requirements of (i) adequate angular resolution (in order to have a wide enough acceptance angle to be able to transmit *all* energetic fragment ions through energy analyzers) and (ii) adequate energy resolution (in order to distinguish between the translational energies of different fragment ions). Constraint (i) requires translational energy spectrometers to be operated with wide slits whereas constraint (ii) requires the use of narrow slits. Moreover, different ion sources, and different operating conditions (viz. gas pressure, anode voltage, plasma density) produce precursor ions with varying amounts of internal energy. In order to minimize experimental uncertainties, the CID studies we report here were conducted under a variety of experimental conditions: (a) using three types of ion sources, (b) different collision energies, (c) light and heavy targets, and (d) three translational energy spectrometers possessing different values of energy and angular resolution.

We have also determined average values of kinetic energies released ($E_k$) when the molecular ion dissociates into either of the two channels, producing $O^+$ and $CO^+$ fragments, and we have compared our results with values deduced by us using contemporary potential energy functions of low-lying electronically excited states of $CO_2^+$. The average $E_k$ values can be interpreted in a manner that is consistent with the measured $CO^+$ to $O^+$ ratio using a curve-crossing model involving excited electronic states of $CO_2^+$.

## II. EXPERIMENTAL METHOD

Our CID experiments were carried out using the ion translational energy spectrometry (TES) method. Application of the TES technique to studies of the dissociation of molecular ions has been described in a number of recent reports (see, for instance, [22], and references therein). In the present study, our CID experiments were carried out on three different ion translational energy spectrometers. In one apparatus (TES1), ions were produced by electron impact in a high-pressure, arc type of ion source. The high pressures used in such a source ensure that collisional deactivation proceeds very efficiently and, as a result, the cation species that are extracted from such a source are predominantly in their ground electronic state. In another apparatus (TES2), ions were produced using a conventional low-pressure, Nier type of ion source; in such a source it is expected that cations would be produced in an unknown mixture of ground and low-lying metastable states. In the first two spectrometers (TES1 and TES2), ions were extracted by an accelerating potential of 1–3 kV. The extracted ions were transported through a cylindrical electrostatic lens assembly to produce a collimated ion beam. Subsequently, a Wien filter (crossed electric and magnetic fields) was used to carry out analysis on the basis of mass-to-charge ratio and an electrostatic energy monochromator was used to produce a monoenergetic ion beam which intersected, in a 90° crossed-beams geometry, a gas jet of neutral target atoms or molecules. Forward scattered collision products were energy analyzed by a second electrostatic energy analyzer. TES1 and TES2 are located in Mumbai. In the third apparatus (TES3, located in Aarhus), ions were produced using yet another type of ion source, a low-pressure Nielsen plasma source. Cations produced in this source were electrostatically accelerated to energies of 50 keV. These energetic ions are magnetically mass selected and directed to a gas cell where they underwent single collisions with target atoms or molecules. After exiting the target cell, the charged fast fragments were energy analyzed using a cylindrical electrostatic energy analyzer. In all three types of apparatus, ion detection was by means of a channel electron multiplier operating in the particle counting mode, coupled to conventional fast electronics and a multichannel analyzer.

Typical gas pressures within the high-pressure ion source used in TES1 were in the $1\times10^{-1}-5\times10^{-2}$ Torr range. Immediately outside the ion source and in the region of the energy analyzers and the detector, the pressure was maintained in the $10^{-8}-10^{-7}$ Torr range by means of fast differential pumping; in the collision region, the number densities in the neutral molecular beam corresponded to pressures in the region of $5\times10^{-4}$ Torr range. In the low-pressure ion source used in TES2, typical working pressures were approximately $1-5\times10^{-6}$ Torr. The plasma source in TES3 was operated at gas pressures of $\sim10^{-3}$ Torr. Typical operating pressures in the remaining part of TES2 and TES3 were in the region of $1\times10^{-7}$ Torr. TES1 used parallel plate electrostatic energy analyzers for monochromation and postcollision analysis of ion kinetic energies. The corresponding analyzers in TES2 were of the 90° cylindrical electrostatic type. In TES3, momentum monochromation of the 50-keV incident beam was achieved with a magnet; an electrostatic hemispherical analyzer was used for postcollision energy analysis.

Details of the three spectrometers can be found in a number of recent publications on the use of TES in studies of dissociation, excitation, and charge stripping processes (TES1 [23–28], TES2 [29,30], TES3 [31]). It is pertinent to make note of the geometrical acceptance angles for product ion energy analysis in the three instruments. In TES1, the distance between the well-defined collision zone (possessing an interaction volume of 1 $mm^3$) and the entrance slit of the postcollision energy analyzer along with the width of this slit were adjusted such that the apparatus had an angular resolution of $4\times10^{-3}$ radians in the dispersing ($x$-$y$) plane and an angular resolution of 0.17 radians in the nondispersing ($x$-$z$) plane. In TES3, the distance between the interaction region and the entrance slit of the electrostatic analyzer was fixed (1 m), but slit widths could be varied, and hence the angular resolution for a given measurement could be chosen. In experiments conducted with an He target, the slit width was adjusted such that the apparatus had an angular resolution of $1\times10^{-4}$ radians in the dispersing plane and $\sim2.5\times10^{-4}$ radians in the nondispersing plane. As the incident $CO_2^+$ ion dissociated in the interaction region in TES1 or in TES3, these geometrical acceptance angles ensured that only the signals of those dissociation products were recorded, which occurred when the O-C-O internuclear axis was parallel to the direction of the incident beam. On the basis of the geometrical configuration of the apparatus (slit widths and distances between the interaction region and the entrance of the postcollision energy analyzer) we computed that the degree of orientation of the incident linear $(\text{O-C-O})^+$ molecular ion that was demanded in the two spectrometers, TES1 and TES3, was $0°\pm9.5°$ and $0°\pm0.01°$, respectively, in the non-energy-dispersing plane and $0°\pm0.24°$ and $0°\pm0.005°$, respectively, in the energy-dispersing plane. The cylindrical energy analyzers (mean radius=55 cm in each case) used in TES2 were focussing devices, with the object and image focal points located at a distance of $\sim$19 cm from the entrance and exit planes, respectively. In this type of instrument it is not easy to directly correlate the geometrical acceptance angle with angular resolution for such focussing devices, but comparisons of measurements carried out in the present study using both TES2 and TES1 of average $E_k$ values and of $E_k$ distributions (as indicated by fragment ion peak shapes) lead us to believe that the angular resolutions were not too different in the two instruments. Implications of this aspect of our experimental design have been discussed in the context of collision-induced dissociation studies elsewhere [25,26,32]; at this juncture it is sufficient to draw attention to the fact that momentum transfer to the target atom or molecule in all our collision systems was negligible. Simple kinematics applied to our zero-degree scattering situation indicates that the recoil imparted to the target was $\leqslant 0.1$ eV in the present measurements.

In TES3, when $C_{60}$ was used as the target gas the entrance slits of the electrostatic analyzer were completely open ($\sim$15 mm) in order to ensure total collection of the fragment ions. The fact that the measured $CO^+$ to $O^+$ ratio was found to remain the same when He and $C_{60}$ were used as targets (with the slit width being 0.2 mm in the former case and being 15 mm in the latter case) suggests minimal energy discrimination and close to 100% collection efficiency as far as fragment ion analysis and detection is concerned.

## III. RESULTS AND DISCUSSION

### A. Translational energy spectra

Figure 1 shows typical translational energy spectra of $CO^+$ and $O^+$ fragments obtained when $CO_2^+$ ions collided with He atoms at an impact energy of 2.5 keV. TES1 was used in this case, with the high-pressure ion source operating in a low-arc-current mode (the mean electron energy being 156 eV, the arc current being 0.02 A, giving rise to a medium-temperature plasma within the source at pressures as high as $10^{-1}$ Torr). In this spectrum, and in the ones to follow (Figs. 2–4), the ratio of $CO^+$ to $O^+$ ions was found to be $\sim$6, which is approximately 20 times higher than what was observed in photoionization experiments [1,4,20,21]. The measured ratio of the $O^+$ to $CO^+$ intensity in these photoionization experiments was $\sim$3, in good agreement with the ratio predicted from the relative populations of vibrationally excited levels of $CO_2^+$ in the *C* state. This ratio was deduced by assuming that all the $CO_2^+$ ions above the dissociation limit yield $CO^+$. All $CO_2^+$ ions formed in the excited vibrational levels of *C* state have, indeed, been shown to dissociate to $CO^+$ in a photoion-photelectron coincidence experiment of Bombach *et al.* [20]. Armenante *et al.* [8] obtained a similar value for the ratio using electrons in place of photons as the ionizing agents. They studied the ratio as a function of the electron energy and found that it increases sharply between 18 eV and 20 eV, which they attributed to possible double collisions, while between 21 eV and 30 eV the ratio falls sharply, which could be due to high-energy states being accessed that can dissociate to both $O^+$ and $CO^+$. Beyond 30 eV, the ratio was observed to remain close to unity since all dissociation channels are open. Thus the dissociation mechanism proposed was that, below the threshold for $CO^+$ formation, most of the $CO_2^+$ ions dissociate to form $O^+$ and CO fragments. As the threshold is passed the $O^+$ yield is quenched and $CO^+$ fragments are exclusively formed. This proposed mechanism was consistent with the results of *ab initio* molecular orbital calculations of low-lying states of $CO_2^+$ [18].

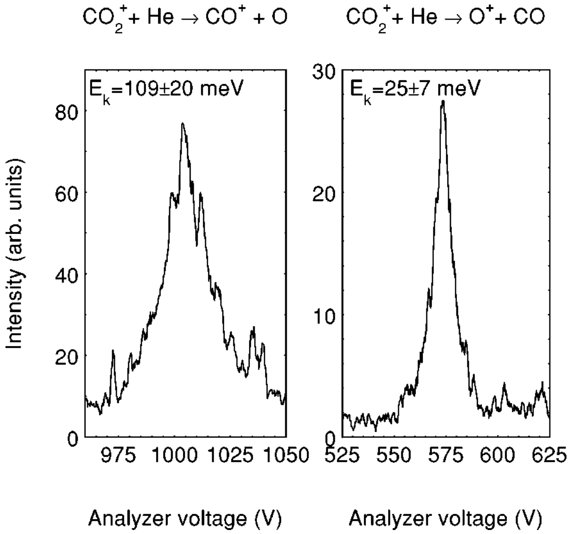

FIG. 1. Translational energy spectra of the products of the dissociation of $CO_2^+$ resulting from collision, at 2.5 keV energy, with He. The spectra were obtained using TES1 with the high-pressure ion source operating in the low-arc-current mode ($I_{arc}=0.02$ A, $V_{anode}=156$ V). The elastically scattered $CO_2^+$ peak appeared at an analyzer voltage ($V_{el}$) of 1586 V. The mean values of the kinetic energy released ($E_k$, in the center-of-mass frame) are indicated for the two channels. The ion intensities are in arbitrary units.

Apart from determining the ratio of different fragment ion peaks, the translational energy spectrum shown in Fig. 1 also enables estimation of the energy loss associated with the dissociation process. In the case of $CO_2^+$ projectiles, if $V_{el}$ is the postcollision analyzer voltage at which the elastically scattered parent ions are transmitted to the ion detector, then $CO^+$ fragments would be expected to be transmitted at an analyzer voltage of $[V_{el}\times(28/44)\text{-}\Delta V]$; the corresponding voltage at which $O^+$ fragment ions are transmitted would be $[V_{el}\times(16/44)\text{-}\Delta V]$. $\Delta V$ is a voltage which accounts for the energy loss associated with the excitation from the ground

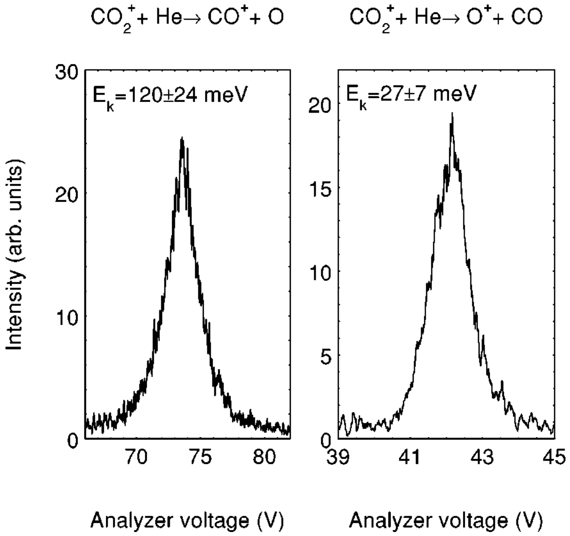

FIG. 2. Collision-induced dissociation of $CO_2^+$ upon impact, at 1.4 keV energy, with He. The translational energy spectra of the two dissociation channels were obtained using TES2 with a conventional, low-pressure, Nier type of electron impact ion source. The elastically scattered $CO_2^+$ peak appeared at an analyzer voltage ($V_{el}$) of 116.3 V. The mean values of the kinetic energy released ($E_k$, in the center-of-mass frame) are indicated for the two channels.

electronic state of $CO_2^+$ to the excited dissociating state $CO_2^{+\star}$. Multiplication of $\Delta V$ with the analyzer constant yields a direct experimental measure of the energy loss; it enables deductions to be made about the highest dissociating electronic state that takes part in the overall dynamics.

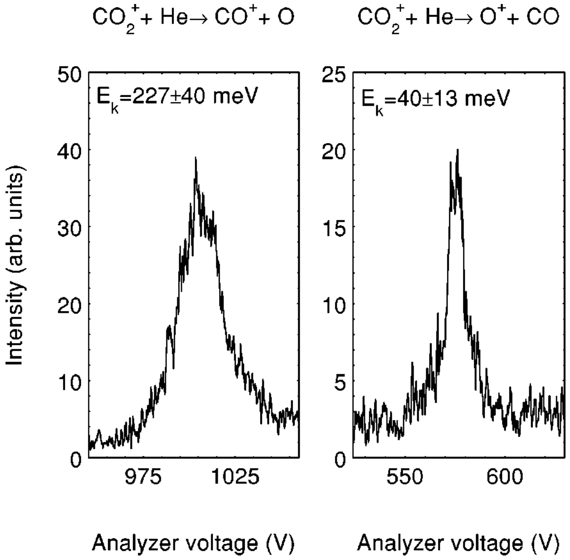

FIG. 3. Translational energy spectra of the products of the dissociation of $CO_2^+$ resulting from collision, at 2.5 keV energy, with He. The spectra were obtained using TES1 with the high-pressure ion source operating in the high-arc-current mode ($I_{arc}=0.25$ A, $V_{anode}=156$ V). The mean values of the kinetic energy released ($E_k$, in the center-of-mass frame) are indicated for the two channels.

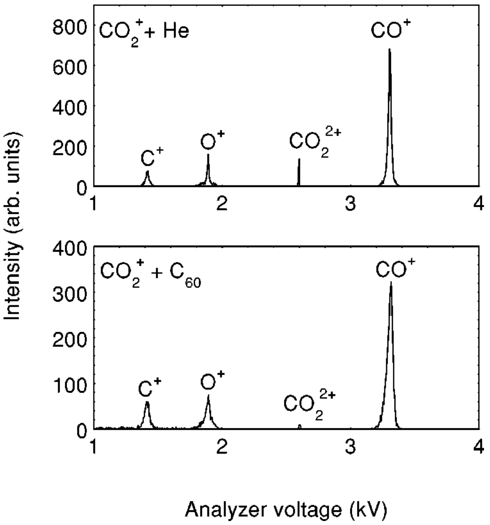

FIG. 4. The top panel shows the translational energy spectrum of the fragment ions when $CO_2^+$ collides with He target at an impact energy of 50 keV; in the spectrum shown in the bottom panel, the target used was $C_{60}$. These spectra were obtained using TES3, the parent $CO_2^+$ ions were produced in a plasma ion source and the mean electron energy was 230 eV.

Although the broad and featureless peaks obtained in TES measurements of CID processes (Figs. 1–3) make it difficult to make measurement of $\Delta V$ with precision, from a very large number of spectra measured in the present experiments we deduce an energy loss value of $\sim 6 \pm 1$ eV. This value suggests that the amount of translational energy converted to potential energy during the collision is sufficiently large for collisional excitation of the projectile $CO_2^+$ ions up to the $C\,^2\Sigma_g^+$ state, which has a vertical excitation energy of 19.4 eV with respect to the $\nu=0$ level of the $X\,^1\Sigma^+$ ground electronic state of neutral $CO_2$. Higher energy electronic states need not, therefore, be invoked in discussion of the present low-impact-energy results.

Figure 2 shows the translational energy spectra measured using TES2 in 1.4 keV collisions between $CO_2^+$ and He; these spectra were obtained using the low-pressure ($\sim 10^{-5}$ Torr), electron impact ion source, with an electron energy of $\sim 100$ eV). Figure 3 shows the translational energy spectra of the fragment ions obtained as a result of 2.5 keV collision between $CO_2^+$ and He in TES1 under high-arc-current conditions (the mean electron energy was still 156 eV, as in the case of the spectra depicted in Fig. 1, but the arc current was tenfold higher, 0.25 A, giving rise to a high-pressure, high-temperature plasma within the ion source). Similar spectra were also obtained at different values of mean electron energy (106 eV and 200 eV), with the arc current being kept at 0.25 A.

Figure 4 shows the translational energy spectra measured using TES3. The top panel shows the fragment ion spectrum obtained as a result of a 50-keV collision between $CO_2^+$ and He (the $CO_2^+$ ions were produced in our ion source operating with an anode voltage of 230 eV). The bottom panel shows the corresponding spectrum of product ions obtained when $CO_2^+$ collided with $C_{60}$ molecules. In both cases, the $CO^+$ to $O^+$ ratio was measured to be $\sim 5$.

All measurements carried out using TES1, TES2, and TES3 confirmed that the $CO^+$ to $O^+$ ratio was $\sim 5-6$ (cf. the corresponding ratio measured in photoionization experiments was, as noted above, ~0.3). Before considering the implications of such a significant difference, it might be of interest to also consider the kinetic energies released upon dissociation of $CO_2^+$ into $CO^+ + O$ and $O^+ + CO$ fragments. It is also of interest to note that evidence for a $CO^+$ to $O^+$ ratio of ~5.5 was also forthcoming from dissociative electron capture measurements carried out in $He^+$-$CO_2$ collisions are impact energies between 9 and 200 eV [33]. Dissociation of $CO_2^+$ ions occurred from the doubly-excited $^2\phi_u$ state, located at an energy of 24.6 eV above the ground electronic state of $CO_2^+$.

### B. Energetics

In spectra measured using TES1 (Figs. 1,3), the half-widths of the peaks relating to $CO^+$ and $O^+$ fragments were of the order of 20 V and 10 V, respectively; the corresponding half-width for the elastically scattered $CO_2^+$ peak (not shown in the spectra) was approximately 0.6 V. In TES2 (Fig. 2), the half-widths of the fragment ion peaks (~3 V for $CO^+$, ~2 V for $O^+$) are much larger than the half-width of the elastically scattered $CO_2^+$ ion beam(~0.3 V). In TES3 (Fig. 4, top panel), the half-widths of the fragment ion peaks were of the order of 24 V, 14 V and 21 V for $CO^+$, $O^+$ and $C^+$, respectively. The peak corresponding to $CO_2^{2+}$ dication formation by a charge stripping process has the same width as the elastically scattered $CO_2^+$ peak (7.6 V). As in the lower-impact-energy case, the broadening observed in fragment ion peaks is caused by the conversion of released dissociation energy into translational energy.

When linear $CO_2^+$ ions fragment, they do so with the internuclear axis having a range of angles with respect to the axis of the translational energy spectrometer and, as discussed above in the context of the instruments' angular acceptance angles, only those incident molecular ions that undergo dissociation such that their O-C-O axes lie within a range of TES acceptance angles fall within the purview of the present experiments. At the center of each of the two fragment ion peaks the energy release values are close to zero: this part of the energy distribution is essentially due to those ions that fragment with their internuclear axes at angles to the TES axis which are close to the maximum acceptance angle in each instrument. The tails of each peak measure the high-energy components of the released energy that result from those dissociation processes that occur when the O-C-O internuclear axes are parallel to the flight path of the molecular ion. Indeed, for large energy releases, the forward and backward moving fragment ions can be readily differentiated (see, for instance [25], for a simulation of trajectories of fragment ions possessing different kinetic energy release components following dissociation of triatomic ions in TES1). Consider the spectra measured using TES1 (Figs. 1,3). The angular acceptance half-angle in TES1 is determined by the 60 mm distance between the $CO_2^+$-He interaction zone and the entrance to the postcollision energy analyzer whose entrance slit had a half-width of 0.25–0.5 mm in the course of the present series of experiments, yielding a geometrical angular resolution of $\pm 0.24° - \pm 0.48°$. For an impact energy of 2.5 keV, $CO^+$ fragments possessing an average $E_k$ value of 90 meV in the center-of-mass frame (total $E_k = 250$ meV) and $O^+$ fragments produced with an average $E_k$ value of 25 meV (total $E_k = 40$ meV), result in laboratory scattering angles of ~0.43° and ~0.3°, respectively. Clearly, TES1 discriminates to some extent against the higher-energy components in the $E_k$ distribution for both fragment ions, but more so for $CO^+$ fragments. Consequently, the $CO^+$ to $O^+$ ratio which we have determined in our present experiments must be regarded as a *lower limit*. In order to obtain a realistic estimate of the distribution of energies released upon dissociation some of our earlier studies have compared simulated trajectories of fragment ions, which possess a range of different energy release values, with measured peak shapes [25,34]. Measurement of the half-width of the fragment ion peak yields an incompletely defined *average* value of the center-of-mass kinetic energy released upon dissociation. Nevertheless, measurements of half-widths have been extensively used in the mass spectrometry of polyatomic ions using single and double focussing instruments in which a determination of angular acceptance angles has been impossible to make. Such average $E_k$ measurements have proved useful in gaining qualitative insight into the dissociation dynamics.

If $E$ is the kinetic energy of, for example, a projectile homonuclear diatomic molecule, and $E_k$ is the average value of the kinetic energy released (in the center of mass) upon dissociation, the measured energy in the laboratory frame, $\epsilon_{lab}$, can be deduced simply by addition of collision velocities:

$$\epsilon_{lab} = E/2 \pm (E_k E)^{1/2} + E_k/2.$$

An amplification of $E_k$ in the laboratory frame occurs in such transformations; this energy ''amplification'' makes it possible to study dissociation processes even in instruments possessing relatively modest energy resolution capabilities and the TES technique has been successfully used to elucidate the role of vibrational [24] as well as rotational [32] states in collision-induced and unimolecular dissociation processes. In the present study we do not concern ourselves with the fine structure observed in the peaks and will focus attention only on the average value of kinetic energy released upon dissociation of $CO_2^+$ into the two dissociation channels.

Despite the significantly different pressure conditions under which $CO_2^+$ ions were formed in TES1 and TES2, the average $E_k$ values deduced from the two spectra were found to be remarkably similar: $109 \pm 20$ meV (TES1) and $120 \pm 24$ meV (TES2) when $CO_2^+$ ions dissociate to $CO^+ + O$. The corresponding $E_k$ values for the $O^+ + CO$ limit were measured to be $25 \pm 7$ meV (TES1) and $27 \pm 7$ meV (TES2). The $E_k$ value of the $CO^+$ fragment changed from $109 \pm 20$ meV to $208 \pm 30$ meV in TES1 when the arc current was enhanced by one order of magnitude (resulting in a much hotter plasma within the ion source). However, $O^+$ fragment ions continued to be produced at essentially thermal energies even under the high-arc conditions. The results obtained from TES3 show that despite the substantially higher collision energy, the average $E_k$ values are not significantly altered. From TES3 data, the $E_k$ value measured for the $CO^+ + O$ channel was $280 \pm 5$ meV and the $E_k$ value of the $O^+$ fragment was found to be $93 \pm 3$ meV. Though

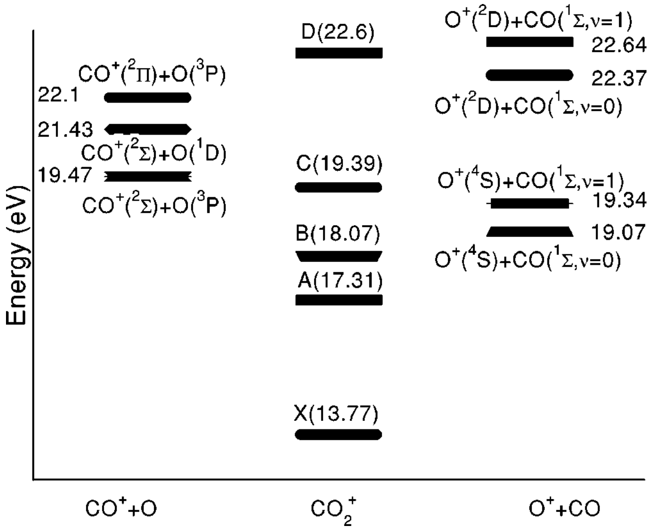

FIG. 5. Overview of low-lying electronic states of $CO_2^+$ and various dissociation limits.

new fragmentation channels open at this collision energy (for instance, production of $C^+$ ions), indicating that higher states are being accessed, the $CO^+$ to $O^+$ ratio remained higher than that observed in photoionization experiments, in accord with the findings from our low-collision-energy experiments using TES1 and TES2. Moreover, the average $E_k$ values deduced from TES3 data were found to be not inconsistent with those obtained using TES1 and TES2.

Unlike the situation that pertained in the photoionization experiments of Eland and co-workers [4,21], where detection of ions in coincidence with the photoelectrons enabled study of well-specified excited states of $CO_2^+$, many electronic states can be populated in the collisional excitation process of the type probed in the present experiments. Figure 5 shows various low-lying electronic states of $CO_2^+$ that can be accessed in TES1 and TES2 experiment (note the discussion on our energy loss measurements) and the relative energetic positions of the dissociation products in different electronic states. Collision-induced dissociation of a molecule, such as a triatomic ion, $ABC^+$, is conventionally understood as a sequential process in which the molecular ion, upon collision with a neutral atom or molecule $M$, is initially excited to a higher electronic state,

$$ABC^+ + M \rightarrow ABC^{+*} + M - Q.$$

The excitation energy $Q$ results from the conversion of the kinetic energy of the projectile ion to its potential energy. The excitation can be to a stable, predissociating, or purely repulsive electronic state of the molecular ion. In the latter two cases, the second stage of the dissociation process occurs when the molecular ion fragments, releasing a range of kinetic energies to the fragments in the center-of-mass frame:

$$ABC^{+*} \rightarrow AB^+ + C + E_k$$

or

$$ABC^{+*} \rightarrow A + BC^+ + E_k.$$

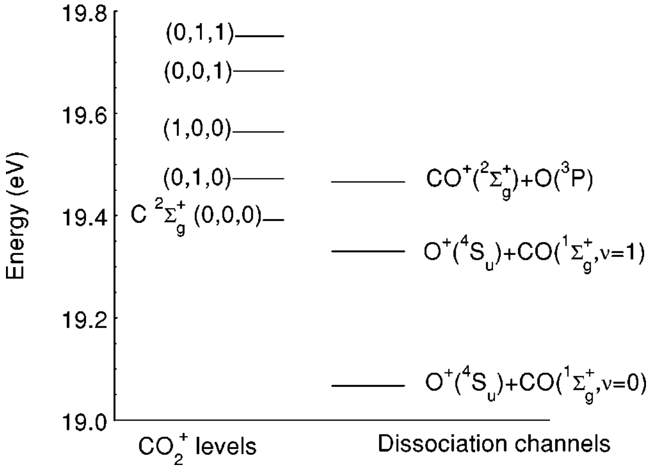

FIG. 6. Vibrational levels of the $C^2\Sigma_g^+$ state of $CO_2^+$ and various dissociation limits.

The energy released in either of these processes is shared between the two fragments in the inverse ratio of their masses and reflects the shape of the potential energy function of the intermediate electronically excited state. As noted above, determination of $Q$ in the course of a large number of measurements carried out using both TES1 and TES2 has indicated that the $C$ state of $CO_2^+$ dominates the dissociation dynamics.

Figure 6 shows the different vibrational levels of the $C$ state of $CO_2^+$ along with possible dissociation channels [21]. It is to be noted that the $CO^+(^2\Sigma)+O(^3P)$ dissociation limit lies 75 meV above the (0,0,0) vibrational level of the $C$ state. Furthermore, below the threshold for $CO^+(^2\Sigma)$ production there are only two dissociation pathways leading to $O^+(^4S)$ production, with the neutral CO $(^1\Sigma)$ fragment being produced either in the ground or the first vibrationally excited state. In the former case, the amount of excess energy that could be carried away by the fragments is 324 meV; the corresponding value in the later case (excitation to the first vibrational level) is 58 meV.

There are two other dissociation channels that can give rise to formation of $O^+$ fragments, and both lie in the vicinity of the $D$ state. Although our energy loss measurements made using TES1 and TES2 offer strong indications that the $D$ state is unlikely to be involved in the overall dynamics, it is of interest to consider the following. The channel leading to $O^+$ $(^2D)$ formation with the accompanying CO $(^1\Sigma)$ fragment in its ground vibrational state lies $\sim$ 230 meV below the $D$ state while the channel leading to $O^+(^2D)$ and CO $(^1\Sigma)$ in its first vibrationally excited state lies $\sim$36 meV above the $D$ state. Consequently, if dissociation of $CO_2^+$ were to somehow take place from the $D$ state, the $E_k$ value for $O^+ + CO$ formation would be expected to be close to either of these energy values. Apart from the $CO^+(^2\Sigma)+O(^3P)$ dissociation limit, which is 75 meV above the ground vibrational level of the $C$ state, there are two more limits, $CO^+(^2\Sigma)+O(^1D)$ and $CO^+(^2\Pi)+O(^3P)$, which lie, respectively, 0.49 eV and 1.16 eV below the $D$ state. So the $E_k$ value associated with formation of $CO^+$ should be in excess of 0.4 eV if dissociation were to take place from this state.

The near-thermal $E_k$ values for $O^+$ fragment ions measured in TES1 and TES2 experiments, irrespective of ion source conditions, are consistent with the postulate that we put forward on the basis of our energy loss measurements that $CO_2^+$ ions dissociate from the $C$ state to produce $O^+$ with the neutral fragment CO in the first vibrationally excited state. It is pertinent to note here that in the photoion-photoelectron experiment carried out by Eland [4], analysis of the $E_k$ values also indicated that 89% of $CO_2^+$ dissociated to produce CO in the first vibrationally excited state. Also, the relatively low values of average $E_k$ that we measured when $CO_2^+$ ions dissociated to form $CO^+$ reinforces our belief that the dissociation essentially takes place from the $C$ state. It is noteworthy that in the first two of our apparatuses, particularly when our ion sources were operated under low-pressure conditions, the average $E_k$ value measured was $\sim 114$ meV, in reasonably good accord with the value of 95 meV, which would be expected if the $CO_2^+$ ions were in the (1,0,0) vibrational level of the $C$ state during the initial collisional excitation process. When the ion source in TES1 was operated under high-pressure conditions, the measured $E_k$ value became $\sim 208$ meV. The amount of excess energy expected to be released if $CO_2^+$ ions were produced in the (0,0,1) vibrational level of the $C$ state is 217 meV, in gratifyingly good accord with our measured value.

Does this observation indicate that there could be collisional excitation to high vibrational levels of the $X$ ground state of $CO_2^+$ within the ion source, which, in turn, is reflected in vibrational excitation of the $C$ state during the subsequent $CO_2^+ + M$ collisional excitation process? This would be contrary to expectations that under high-pressure conditions in the TES1 ion source it is collisional *deactivation* that is the dominant process.

Our analysis so far has been carried out under the assumption that there is negligible rotational excitation of the diatomic fragment. The only experimental evidence for such rotational excitation is somewhat tentative, and it emanates from a comparison of fragment ion $E_k$ values deduced from the photoionization experiments of Eland [4] and Bombach *et al.* [20]. The following average $E_k$ values for the formation of $O^+$ were measured in the latter experiments: with CO being formed in the $\nu=0$ or 1 vibrational level from $CO_2^+$ in the ground vibrational level of the $C$ state, the average $E_k$ values were $130 \pm 50$ meV (for $\nu=0$) and $20 \pm 10$ meV (for $\nu=1$). The branching ratios for $\nu=0$ and $\nu=1$ were measured to be 0.56 and 0.38, respectively. Similarly, when the $CO_2^+$ ions, prepared either in the (1,0,0) or the (0,1,1) vibrational level of the $C$ state, dissociated to form $CO^+$, the $E_k$ values measured were, respectively, $45 \pm 20$ meV and $170 \pm 50$ meV; the corresponding branching ratios were 1 and 0.67 [20]. In the experiments of Eland [4], however, significantly different branching ratios were found. By comparing his measured TOF spectrum with one that was simulated using Monte Carlo techiques (with $E_k$ values being the fitting parameters), Eland deduced branching ratios of 0.15 and 0.85 for average $E_k$ components of $O^+$ of 130 meV and 57 meV, respectively. No rotational excitation was allowed for in these simulations. Indeed, Bombach *et al.* [20] found that the use of Eland's branching ratios in their simulations resulted in very bad agreement with measured spectra and they speculated that the reason for this disagreement might be that CO fragments are produced in rotationally excited states.

The role of rotational excitation in the dissociation dynamics of molecular ions has been noted in earlier TES experiments [32]. In the case of CID of $CO_2^+$ ions, such excitation is consistent with the scenario for the dissociation dynamics that is discussed below in terms of curve crossings: rotational excitation is the preferred mode for mediation in internal conversion from, say, an $A_1$ state to a $B_1$ state as interaction of $B_1$ symmetry is required and no vibration belongs to this species in a bent triatomic molecule.

In view of the conflicting nature of the average $E_k$ values measured in two photoionization experiments, it is of interest to note that the $E_k$ values measured for the $CO^+ + O$ and $O^+ + CO$ channels when $CO_2^+$ ions undergo collision-induced dissociation have been measured in an earlier experiment using a conventional low-pressure Nier type of electron impact ion source. At considerably higher values of impact energy (8 keV) than in our first two experiments, average $E_k$ values were determined to be 169 and 30 meV, respectively, for the $CO^+ + O$ and $O^+ + CO$ channels [13].

In the present experiments we also made a series of measurements at different values of electron energy within the ion sources in both TES1 and TES2 to explore whether $CO_2^+$ ions that might be produced in electronically excited states might yield dissociation dynamics that were different. We observed that the fragment ion peak shapes (and, hence, the gross distribution of $E_k$ values) and the ratio of $CO^+$ to $O^+$ remained essentially the same, irrespective of the values of electron energies in the two types of ion sources employed in the present experiments. This lends strong credence to our belief that the $CO_2^+$ ions are predominantly produced in the ground $X$ state in both TES1 and TES2 in our experiments and that dissociation dynamics essentially involves only the $C$ state.

### C. $CO^+$ to $O^+$ ratio

Having used the results of energy loss measurements to establish some support for the conjecture that collisional dissociation to different product states appears to predominantly take place from the $C$ state of $CO_2^+$ (and our $E_k$ measurements are not inconsistent with this conjecture), can one now rationalize the measured $CO^+$ to $O^+$ ratio?

Figure 7 shows a correlation diagram valid for linear geometry of the $CO_2^+$ ion. Some of the relevant electronically excited states which may be involved in the production of the observed fragments are shown. From the figure it is clear that $O^+$ and $CO^+$ can be produced by any of the three levels $^4\Sigma$, $^4\Pi$, and $^2\Pi$, provided that dissociation takes place such that the linear geometry of the ground electronic state of $CO_2^+$ is preserved. The $C$ state is predissociated by a low-lying quartet state ($a\,^4\Pi_u$), which lies 1.2 eV above it. These two states cross each other when the O-C-O angle is 160°, resulting in a possible intersystem crossing. The efficiency for such a crossing was shown to be low [18] because the predominant configurations of these two states are diexcited with respect to each other. When in a more stable bent geometry (the energy minimum being at 120°) the $a$ state undergoes a further, more efficient, intersystem crossing with the ground $X$ state. Once in the $X$ state the system dissociates

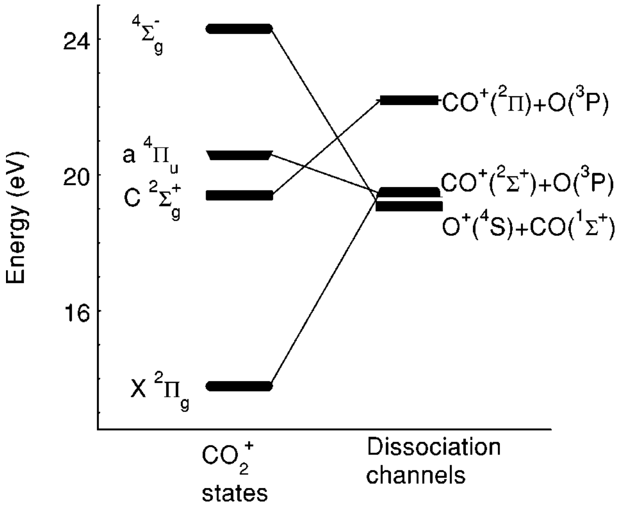

FIG. 7. Correlation diagram linking various low-lying electronic states of $CO_2^+$ to different dissociation limits.

into the relevant asymptote, giving rise to $CO^+$ ions. Although there is a curve crossing between the $X$ and $^4\Sigma$ states in the linear geometry the $O^+$ ions cannot be formed due to negligible spin-orbit coupling.

In Fig. 8 we attempt to represent the dynamics in pictorial fashion. In the linear geometry, the $^4\Sigma^-$ state correlates to the $O^+ + CO$ dissociation limit and crosses the $a^4\Pi$ state at $r_{CO} = 1.35$ Å (the other C-O internuclear distance being kept fixed at 1.128 Å, the equilibrium internuclear separation in carbon monoxide). In the linear geometry there is adiabatic interaction between these two states of different symmetry and multiplicity. However in the bent geometry, these two states belong to the same $^4A''$ symmetry representation, and nonadiabatic interaction in the form of an avoided crossing becomes possible. So, when the potential surfaces of these two states are plotted, as in Fig. 8, as a function of the internal degrees of freedom (the C-O bond length and the O-C-O angle), they are degenerate at one point only, and everywhere else they repel each other. The resulting surface is a double cone with its apex at the point of degeneracy. Such a conical intersection is depicted in Fig. 9 where the two surfaces cross at a common apex at $r_{CO} = 1.35$ and an O-C-O angle of 180°. As shown in the figure, the lower sheet of the cone, which is the potential energy surface of the lowest $a^4\Pi$ state, correlates with the $O^+(^4S) + CO(^1\Sigma^+)$ dissociation limit, *but only in the bent geometry.*

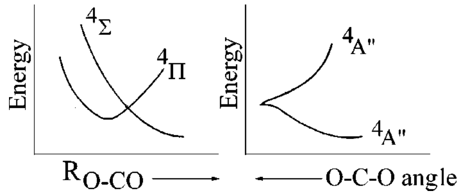

FIG. 8. Potential energy functions for the lowest quartet states of $CO_2^+$ plotted as a function of O-CO internuclear distance (left panel) and O-C-O angle (right panel). In the former case, the O-C-O angle is frozen at 180° and the other O-CO distance is frozen at the equilibrium internuclear separation of the ground electronic state of CO (1.128 Å). In the right panel, one C-O internuclear distance is fixed at 1.128 Å and the other at 1.38 Å.

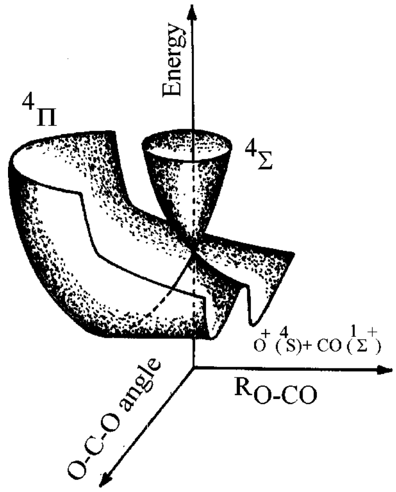

FIG. 9. Conical intersection resulting from the accidental degeneracy of the $^4\Pi$ and $^4\Sigma$ potential energy surfaces shown in Fig. 8 (see text).

The dissociation dynamics of the $CO_2^+$ ion is, therefore, capable of being rationalized using the conical intersection picture in the following fashion. The population in the $C$ state undergoes a slow intersystem crossing to the quartet $a$ state that is more stable in the bent geometry. Once in the bent geometry, the system relaxes due to the conical intersection between the $a$ and $^4\Sigma$ states and, as a result, $O^+$ fragment ions are formed. If, on the other hand, a further intersystem crossing with the $X$ state takes place, formation of $CO^+$ fragment ions becomes possible, but this process demands that the entire dynamics occurs in the linear geometry.

Since in collisions selective excitation to specific electronic or rovibrational states is not possible, it may be postulated that apart from accessing the ground vibrational level of the $C$ state, rovibrationally excited levels are also accessed. Indications for this have been obtained in the $E_k$ measurements made in the present experiments. Moreover, it has been noted that $CO_2^+$ ions in excited vibrational levels of the $C$ state yield only $CO^+$ fragment ions. But the large abundance of $CO^+$ fragments still cannot be explained since $CO_2^+$ ions in the ground vibrational level of the $C$ state should produce energetically favored $O^+$ ions unless one assumes that in collisional excitation *all* ions are vibrationally excited, a conjecture that is difficult to support on both experimental and theoretical grounds. We carried out our experiments over a range of $CO_2^+$-$M$ impact energies in order to account for any possiblity of collisional excitation of the projectile $CO_2^+$ ions to different electronic and/or rovibrational states, giving rise to possible changes in the $CO^+$ to $O^+$ ratio. We also carried out experiments at different values of the electron energy within our three ion sources, to account for any possiblity of $CO_2^+$ ions being formed in different excited states which, upon collision with $M$, might undergo CID in different fashion, hence resulting in a different $CO^+$ to $O^+$ ratio. However, in our protracted series of CID experiments using three spectrometers, we observed that the $CO^+$ to $O^+$ ratio remained independent of both impact energy (at least in the range 1–5 keV and at 50 keV) as well as electron energy in the ion source (in the range of $\sim 20-250$ eV).

So, how do we rationalize the $CO^+$ to $O^+$ ratio measured in the present series of experiments? We postulate that the apparent enhancement of $CO^+$ intensities that we observe in our collision experiment can be explained when dissociation takes place only in the $C_{\infty v}$ symmetry point group. Under such circumstances, the intersystem crossing of the $C$ state with the vibrational continuum of the $X$ state leads exclusively to formation of $CO^+$ fragment ions.

## IV. CONCLUDING REMARKS

CID experiments have been conducted on $CO_2^+$ ions under a variety of experimental conditions: (i) using three types of ion sources, (ii) different collision energies, (iii) using light and heavy targets, and (iv) using apparatuses possessing different values of energy and angular resolution. Results of all these collision experiments appear to establish that collision-induced dissociation dynamics is remarkably different from that obtained in photoionization experiments. Although the $O^+ + CO$ channel is energetically the lowest dissociation pathway, dissociation into $CO^+ + O$ is found to be the preferred channel in our collision experiments. This is rationalized by considering the conical intersection that results from the accidental degeneracy of the lowest-energy $a^4\Pi$ and $^4\Sigma_g^-$ potential energy surfaces of $CO_2^+$ : the population in the $C^2\Sigma_g^+$ state undergoes a slow intersystem crossing to the quartet $a$ state that is more stable in the bent geometry. Once in the bent geometry, the system relaxes due to the conical interaction between the $a$ and $^4\Sigma$ states and, as a result, $O^+$ fragment ions are formed. If, on the other hand, a further intersystem crossing with the $X$ state takes place, formation of $CO^+$ fragment ions becomes possible, but this process demands that the entire dynamics occurs in the linear geometry.

Our measurements of the ratio $CO^+$ to $O^+$ are found to be substantially higher than results of photoionization experiments. This is indicative of the fact that collision-induced dissociation of $CO_2^+$ ions appears to take place only in the $C_{\infty v}$ symmetry point group. Under such circumstances, the intersystem crossing of the $C$ state with the vibrational continuum of the $X$ state leads almost exclusively to formation of $CO^+$ fragment ions, thereby enhancing the $CO^+$ to $O^+$ ratio.

The average kinetic energies released upon dissociation to different channels of those $CO_2^+$ ions whose internuclear axis is nearly parallel to the axes of the two spectrometers have been measured and are in accord with calculated values. It would be of interest to extend such experiments to other triatomic molecules for which experimental information exists on photon-induced dissociative ionization: differences in the dissociation dynamics pertaining to photon-induced processes and collision-induced ones clearly exist, and may be not only of intrinsic interest but may also be of importance in various applications concerned with plasma processing chemistry and in the atmospheric sciences. To this end, experimental work on the valence isoelectronic ion, $CS_2^+$ has been initiated in our laboratories.

## ACKNOWLEDGMENTS

Experiments using TES1 and TES2 were conducted in the laboratories of the Atomic and Molecular Sciences group at TIFR, Mumbai, and were supported by the Tata Institute of Fundamental Research. Experiments using TES3 were conducted at the laboratories of the Aarhus Center for Advanced Physics (ACAP), funded by the Danish National Research Foundation. Paul Mathur is thanked for implementing some of the computer data-handling procedures.

---

[1] K. E. McCulloh, J. Chem. Phys. **59**, 4250 (1973).

[2] A. Crowe and J. W. McConkey, J. Phys. B **7**, 349 (1974).

[3] M. J. Hubin-Franskin, J. Delwiche, and P. M. Guyon, Z. Phys. D **5**, 203 (1987).

[4] J. H. D. Eland, Int. J. Mass Spectrom. Ion Phys. **9**, 397 (1972).

[5] C. R. Brundle and D. W. Turner, Int. J. Mass Spectrom. Ion Phys. **2**, 195 (1969).

[6] G. R. Kumar, C. P. Safvan, F. A. Rajgara, and D. Mathur, J. Phys. B **27**, 2981 (1994).

[7] G. R. Kumar, P. Gross, C. P. Safvan, F. A. Rajgara, and D. Mathur, Phys. Rev. A **53**, 3098 (1996).

[8] M. Armenante, R. Cesaro, V. Santoro, N. Spinelli, F. Vanoli, G. Del Re, A. Peluso, and S. Filippi, Int. J. Mass Spectrom. Ion Phys. **87**, 41 (1989).

[9] H. M. Rosenstock and C. E. Melton, J. Chem. Phys. **26**, 314 (1957).

[10] R. G. Cooks, *Collision Spectroscopy* (Plenum, New York, 1978).

[11] J. Durup, P. Fournier, and P. Dong, Int. J. Mass Spectrom. Ion Phys. **2**, 311 (1969).

[12] J. H. Beynon, M. Bertrand, E. G. Jones, and R. G. Cooks, J. Chem. Soc. Chem. Commun. 341 (1972).

[13] K. C. Kim, M. Uckotter, J. H. Beynon, and R. G. Cooks, Int. J. Mass Spectrom. Ion Phys. **15**, 23 (1974).

[14] W. von Niessen, G. H. F. Diercksen, and L. S. Cederbaum, J. Chem. Phys. **67**, 4124 (1977).

[15] W. B. England, B. J. Rosenberg, P. J. Fortune, and A. C. Wahl, J. Chem. Phys. **65**, 684 (1976).

[16] W. Domcke, L. S. Cederbaum, J. Schirmer, W. von Niessen, C. E. Brion, and K. H. Tan, Chem. Phys. **40**, 171 (1979).

[17] P. Roy, I. Nenner, P. Millie, P. Morin, and D. Roy, J. Chem. Phys. **84**, 2050 (1982).

[18] M. Th. Praet, J. C. Lorquet, and G. Raseev, J. Chem. Phys. **77**, 4611 (1982).

[19] A. W. Potts and G. H. Fattahallah, J. Phys. B **13**, 2545 (1980).

[20] R. Bombach, J. Dannacher, J.-P. Stadelmann, and J. C. Lorquet, J. Chem. Phys. **79**, 4214 (1983).

[21] J. H. D. Eland and J. Berkowitz, J. Chem. Phys. **67**, 2782 (1977).

[22] V. R. Marathe and D. Mathur, in *Physics of Ion Impact Phe-*

*nomena*, edited by D. Mathur (Springer-Verlag, Berlin, 1991), Chap. 8.

[23] D. Mathur, F. A. Rajgara, and V. Krishnamurthi, Proc.-Indian Acad. Sci., Chem. Sci. **104**, 509 (1991).

[24] G. R. Kumar, V. Krishnamurthi, and D. Mathur, Rapid Commun. Mass Spectrom. **7**, 734 (1993).

[25] G. R. Kumar, L. Menon, and D. Mathur, Phys. Rev. A **48**, 1257 (1993).

[26] M. Krishnamurthy and D. Mathur, Chem. Phys. Lett. **216**, 203 (1993).

[27] D. Mathur, F. A. Rajgara, and C. Badrinathan, Phys. Rev. A **42**, 5282 (1990).

[28] M. Krishnamurthy and D. Mathur, J. Phys. B **27**, 1177 (1994).

[29] M. Krishnamurthy and D. Mathur, Rapid Commun. Mass Spectrom. **9**, 344 (1995).

[30] D. Mathur and M. Krishnamurthy, in *Physics of Electronic and Atomic Collisions*, edited by L. J. Dubé, J. W. McConkey, C. E. Brion, and J. B. A. Mitchell (AIP, New York, 1995), p. 587.

[31] H. Shen, P. Hvelplund, D. Mathur, A. Barany, H. Cederquist, N. Selberg, and D. C. Lorents, Phys. Rev. A **52**, 3847 (1995).

[32] V. Krishnamurthi, D. Mathur, and G. T. Evans, Rapid Commun. Mass Spectrom. **5**, 557 (1991).

[33] M. R. McMillan and M. A. Coplan, J. Chem. Phys. **71**, 3063 (1979).

[34] D. Mathur and J. H. D. Eland, Int. J. Mass Spectrom. Ion Processes **114**, 123 (1992).